Cooperative effect of ribosomal protein s19 and Pim-1 kinase on murine c-Myc expression and myeloid/erythroid cellularity

Anne-Sophie Fröjmark, Jitendra Badhai, Joakim Klar, Maria Thuveson, Jens Schuster and Niklas Dahl

Department of Genetics and Pathology, the Rudbeck Laboratory, Uppsala University, 751 85 Uppsala, Sweden

Correspondence: Prof. Niklas Dahl, Department of Genetics and Pathology, the Rudbeck Laboratory, Uppsala University and University Hospital, S-751 85 Uppsala, Sweden.

e-mail: niklas.dahl@genpat.uu.se

Diamond Blackfan anemia (DBA) is a bone marrow failure syndrome associated with heterozygous mutations in the ribosomal protein S19 (*RPS19*) gene in a subgroup of patients. One of the interacting partners with RPS19 is the oncoprotein PIM-1 kinase. We intercrossed *Rps19*$^{+/-}$ and *Pim-1*$^{-/-}$ mice strains to study the effect from the disruption of both genes. The double mutant (*Rps19*$^{+/-}$*Pim-1*$^{-/-}$) mice display normal growth with increased peripheral white- and red blood cell counts when compared to the w.t. mice (*Rps19*$^{+/+}$*Pim-1*$^{+/+}$). Molecular analysis of bone marrow cells in *Rps19*$^{+/-}$*Pim-1*$^{-/-}$ mice revealed up-regulated levels of c-Myc and the anti-apoptotic factors Bcl_2, Bcl_{XL} and Mcl-1. This is associated with a reduction of the apoptotic factors Bak and Caspase 3 as well as the cell cycle regulator p21. Our findings suggest that combined Rps19 insufficiency and Pim-1 deficiency promotes murine myeloid cell growth through a deregulation of c-Myc and a simultaneous up-regulation of anti-apoptotic Bcl proteins.

Key words: Rps19, Pim-1, erythropoiesis, myelopoiesis, c-Myc, apoptotic factors

Introduction

Diamond-Blackfan anemia (DBA) is a rare bone marrow failure characterized by an absence or decrease of erythroid precursor cells in the bone marrow but otherwise normal cellularity [1,2]. In DBA, as in several bone marrow failure syndromes, affected individuals have an increased risk for developing malignant disease, specifically myelodysplastic syndromes (MDS) and acute myeloid leukemia (AML) [1,3,4]. Approximately 25% of patients with DBA are heterozygous for mutations in the ribosomal protein *S19* gene (*RPS19*) [5] and another 10-20% of patients carry mutations in different ribosomal protein genes [6] RPS19 deficiency in hematopoietic cells is associated with reduced erythroid proliferative capacity [7], mitotic arrest in the G_0/G_1 phase and increased apoptosis of erythroid progenitors [8]. Impaired ribosomal biogenesis is a distinct feature in the pathophysiology of DBA but the connection to erythroid hypoplasia and the predisposition to myeloproliferative disease is unclear [9,10]. It is assumed that the progression to MDS and leukemia requires additional mutations to reach clonal dominance [11]. Several factors interact with RPS19 [12] one of which is identified as the serine-threonine kinase PIM-1 [13]. PIM-1 is ubiquitously present and highly expressed in hematopoietic tissues [14] where it promotes cell cycle progression, cell proliferation and survival [15,16]. The PIM-1 deficient mouse is characterized by microcytotic anemia and impaired erythroid colony forming capacity *in vitro* [17,18]. PIM-1 is also recognized as a synergistic partner with c-Myc in tumorigenesis [19] and the transcriptional activity of c-Myc is dependent on histone phosphorylation by PIM-1 [20]. Moreover, PIM-1 phosphorylates the Cdc25A cell cycle phosphatase, which is a transcriptional target of c-Myc. This links PIM-1-mediated mitogenic signals to the cell cycle machinery [21]. On the other hand, PIM-1 can stimulate c-Myc-mediated apoptosis via activation of caspase-3-like proteases downstream of c-Myc [22]. The proto-oncogene c-Myc has a pivotal role in growth control, differentiation and apoptosis. c-Myc can directly promote ribosome biogenesis and protein synthesis rate through

transcription of several components in the translational machinery [23]. This seems to be counteracted by the ribosomal protein L11 which suppresses c-Myc activity [24].

We have previously generated a mouse model with targeted disruption of *Rps19* [25]. The *Rps19* null mouse is lethal prior to implantation whereas the *Rps19* heterozygous mice show a normal phenotype [25]. To clarify the significance of the previously reported RPS19 and PIM-1 interaction we generated mice with targeted disruptions of *Rps19* and/or *Pim-1*. We present herein the results from the morphological and molecular analysis of hematopoietic organs in these mice strains. Our findings support a combined effect of Rps19 and Pim-1 mutations on myeloid proliferation.

Materials and methods

Generation of mice carrying Rps19 and Pim-1 disruptions

Rps19$^{+/-}$ mice [25] were bred with *Pim-1*$^{-/-}$ mice [18] for several generations on a C57/Bl6 background to produce offspring with the genotypes *Rps19*$^{+/+}$*Pim-1*$^{+/+}$, *Rps19*$^{+/-}$*Pim-1*$^{+/+}$, *Rps19*$^{+/+}$*Pim-1*$^{-/-}$ and *Rps19*$^{+/-}$*Pim-1*$^{-/-}$ (n=83). Breeding was approved by the Uppsala Animal Research Ethics Board (Dnr C256/4). Mice were genotyped by PCR as described previously [18,25] (primer sequences are available upon request).

Hematological analysis and bone marrow preparations

Hematological analysis including hemoglobin concentration (Hb), red- and white blood cell count (RBC, WBC), hematocrit (HC), mean erythroid corpuscular volume (MCV) and mean erythroid hemoglobin concentration (MCHC) was performed using peripheral blood (EDTA) from adult *Rps19*$^{+/+}$ *Pim-1*$^{+/+}$, *Rps19*$^{+/-}$ *Pim-1*$^{+/+}$, *Rps19*$^{+/+}$ *Pim-1*$^{-/-}$ and *Rps19*$^{+/-}$ *Pim-1*$^{-/-}$ mice as previously described[26]. BM cells were collected from *Rps19*$^{+/+}$ *Pim-1*$^{+/+}$ n=9, *Rps19*$^{+/-}$

Pim-1$^{+/+}$ n=8, *Rps19*$^{+/+}$ *Pim-1*$^{-/-}$ n=10 and *Rps19*$^{+/-}$ *Pim-1*$^{-/-}$ n=6 and pooled. In brief, mice femurs were dissected and flushed with +4°C 1xPBS. Following centrifugation at 2000 g for 5 minutes at +4°C BM cells were resuspended in RIPA lysis buffer (50mM Tris-HCl pH 7.5, 150mM NaCl, 1% Triton X-100, 1% sodium deoxycholate and 0.1% SDS) supplemented with proteasome inhibitor MG132 (1:1 000, SIGMA), phosphatase inhibitor cocktail 1 (1:1 000, SIGMA), 0.1 mM Sodium vanadate (SIGMA) and protease inhibitor cocktail (1:1 000, SIGMA). BM proteins were stored at -20ºC.

Histopathological analysis of bone marrow and spleen

BM cells were scraped from mice femurs and BM smears were prepared directly in 100% fetal bovine serum (FBS, GIBCO. Smears were dried in room temperature before Giemsa staining according to standard procedures. Mice spleens were dissected and fixed in 4 % formalin over night before paraffin embedding. Embedded spleens were sectioned and stained with hematoxylin and eosin according to standard procedures.

Western Blotting

Total BM proteins were separated on 10 % SDS-polyacrylamide gels (Invitrogen) and electrophoretically transferred to PVDF Immobilon-FL membranes (Millipore). Non-specific binding was blocked by 1 h incubation with 2% bovine serum albumin (BSA) in PBST (0.1% Tween-20 in 1xPBS). Blots were probed with the primary antibodies beta actin (Abcam), Bak (Sigma), Bcl_2 (Santa Cruz), Bcl_{XL} (Santa Cruz), Cleaved Caspase 3 (Cell Signaling), c-Myc (Santa Cruz), Mcl-1 (Santa Cruz), p21 (Santa Cruz), p53 (Cell Signaling), phosphotyrosine (Upstate Biotechnology) and RPS19 (kindly provided by Prof. Fabrizio Loreni, Italy) for 1 h in a buffer containing 1% BSA in PBST. After being washed for 3x5 minutes in PBST, blots were incubated with Alexa Flour 680 (goat anti-rabbit, Molecular Probes) and IRD-800

(rabbit anti-mouse, LI-COR Bioscience) conjugated secondary antibodies for 1 h. Following washing for 3x5 minutes in PBST and 1x5 minutes in 1xPBS proteins were visualized and quantified using the Odyssey infrared imaging system® and software (LI-COR Bioscience). All proteins are measured at least twice and normalized to beta-actin levels.

Reverse transcription and quantitative real time PCR

Red blood cells in the BM samples were lyzed by EasyLyse erythrocyte lysis buffer (Universal Biologicals). Total RNA was prepared using TRIzol reagent (Invitrogen) according to the manufacturer's recommendations. cDNA was synthesised using a RevertAid^{TM} H Minus First Strand cDNA Synthesis Kit (Fermentas) according to manufacturers protocol. Quantitative real time PCR was performed to analyze *Rps19* and *Pim-1* transcript levels using the Platinum® SYBR® Green qPCR SuperMix-UDG kit (Invitrogen) according to manufacturers recommendations. Primer sequences are available upon request.

Statistical analysis

Results are presented as means ± standard deviation. Western blot experiments were conducted on pooled material. Quantitative real time PCR experiments were set up in triplicates. Each experiment was repeated at least twice. Cell cycle experiments were repeated four times. Results were tested for statistical significance using the two-tailed unpaired Student *t*-test. $P < 0.05$ was considered statistically significant [27].

Results

Mice with a combined Rps19 and Pim-1 disruption have an increased myeloid/erythroid cellularity

To investigate the functional effect of Rps19 and Pim-1 we generated different combinations of *Rps19* and *Pim-1* genotypes by interbreeding the mice strains *Rps19*$^{+/-}$ C57BL/6J, *Pim-1*$^{-/-}$ FVB/NJ and wild type C57BL/6J on a pure C57 background. Litters were genotyped showing a Mendelian distribution (data not shown) for the six possible genotypes. We selected mice with the following genotypes for further analysis: *Rps19*$^{+/+}$ *Pim-1*$^{+/+}$ (n=22), *Rps19*$^{+/-}$ *Pim-1*$^{+/+}$ (n=13), *Rps19*$^{+/+}$ *Pim-1*$^{-/-}$ (n=25) and *Rps19*$^{+/-}$ *Pim-1*$^{-/-}$ (n=23). The growth and weight was measured at age 6 weeks, with no significant differences between the four groups. None of the four groups showed any macroscopic abnormalities and the groups showed a similar survival rate up to the age of analysis (6-8 weeks). We were not able to show a reduction of *Rps19* transcript levels in the *Rps19*$^{+/-}$ *Pim-1*$^{+/+}$ and *Rps19*$^{+/-}$ *Pim-1*$^{-/-}$ mice as previously described [25] (data not shown). *Pim-1* transcript levels were fully knocked down in the *Rps19*$^{+/+}$ *Pim-1*$^{-/-}$ and *Rps19*$^{+/-}$ *Pim-1*$^{-/-}$ mice as expected (data not shown).

Functional consequences of the targeted genes were further assessed in peripheral blood. We analyzed the standard parameters Hb, RBC, EVF, MCV, MCHC and WBC (table 1) from a total of 83 adult mice (*Rps19*$^{+/+}$ *Pim-1*$^{+/+}$ (wild type. n=22), *Rps19*$^{+/-}$ *Pim-1*$^{+/+}$ (n=13), *Rps19*$^{+/+}$ *Pim-1*$^{-/-}$ (n=25) and *Rps19*$^{+/-}$ *Pim-1*$^{-/-}$(n=23)). RBC and WBC were found significantly increased in double mutant mice (*Rps19*$^{+/-}$ *Pim-1*$^{-/-}$) when compared to wild type mice (table 1). No significant differences were found for RBC or WBC when comparing either of the single *Rps19*$^{+/-}$ or the *Pim-1*$^{-/-}$ disruptions to the wild type mice. Microcytosis was previously associated with Pim1 deficiency and found to be similar in the single *Pim-1*$^{-/-}$ mutant mice as well as the double mutant mice (*Rps19*$^{+/-}$ *Pim-1*$^{-/-}$). The Hb levels were subnormal in the

double mutant *Rps19*$^{+/-}$ *Pim-1*$^{-/-}$ mice but significantly increased when compared to the Pim-1 deficient mice (table1). Similarly, the hematocrit was subnormal in the double mutant mice but significantly increased when compared to the single *Pim-1* mutant mice. MCHC showed a tendency towards lower levels in the double mutant mice compared to the *Pim-1* null mutant mice and the wild type but the variations are large within groups and no significant differences were detected. There were no histopathological differences when analyzing the BM and spleen (data not shown)

Rps19 and Pim-1 have a combined effect on cell cycle regulators

To further clarify the increased peripheral cellularity we analyzed the levels of the cell cycle regulators c-Myc and p21 as well as the tumor suppressor protein p53. BM cells were harvested from murine femurs and proteins were prepared and subjected to Western blot analysis. After correlation to beta-actin levels we detect a significant up-regulation of c-Myc ($p<0.01$) levels in the double mutant (*Rps19*$^{+/-}$ *Pim-1*$^{-/-}$) mice when comparing to the three other groups and a significant down-regulation of p21 ($p<0.05$) levels in the *Rps19*$^{+/-}$ *Pim-1*$^{-/-}$ mice when comparing to *Rps19*$^{+/+}$ *Pim-1*$^{+/+}$ mice (Figure 1A-B). When analyzing the levels of p53 we do not detect any differences between the four different groups (Figure 1C).

Combined disruption of Rps19 and Pim-1 alters the levels of apoptotic factors

We next analyzed apoptotic factors in BM cells to substantiate the findings from the cell cycle regulators. We selected anti-apoptotic markers (Bcl_2, Bcl_{XL} and Mcl-1) and apoptotic markers (Bak and cleaved Caspase 3) for analysis by Western blot. We detect a significant up-regulation of the anti-apoptotic markers Bcl_2 ($p<0.05$) and Mcl-1 ($p<0.05$) in the double mutant (*Rps19*$^{+/-}$ *Pim-1*$^{-/-}$) mice when comparing to *Rps19*$^{+/+}$ *Pim-1*$^{+/+}$ and *Rps19*$^{+/-}$ *Pim-1*$^{+/+}$ mice, respectively (Figures 2A and B). Similarly, we find a significant up-regulation in Bcl_{XL}

($p<0.05$) in the double mutant (*Rps19*$^{+/-}$ *Pim-1*$^{-/-}$) mice when comparing to *Rps19*$^{+/+}$ *Pim-1*$^{+/+}$ mice (Figure 2C). We also detect a significant down-regulation of the apoptotic marker Bak ($p<0.001$) when comparing the double mutant (*Rps19*$^{+/-}$ *Pim-1*$^{-/-}$) mice to the other three groups, (Figure 2D) after normalization to beta-actin. Similarly, we find a significant down-regulation of cleaved Caspase 3 ($p<0.05$) in the double mutant (*Rps19*$^{+/-}$ *Pim-1*$^{-/-}$) mice when comparing to *Rps19*$^{+/+}$ *Pim-1*$^{+/+}$ and *Rps19*$^{+/+}$ *Pim-1*$^{-/-}$ mice, respectively (Figure 2E).

Discussion

To investigate the function of the RPS19 and PIM-1 interaction we generated different combinations of *Rps19* and *Pim-1* genotypes by interbreeding the *Rps19*$^{+/-}$ and *Pim-1*$^{-/-}$ mice strains [18,25]. None of the four selected groups (*Rps19*$^{+/+}$ *Pim-1*$^{+/+}$, *Rps19*$^{+/-}$ *Pim-1*$^{+/+}$, *Rps19*$^{+/+}$ *Pim-1*$^{-/-}$ and *Rps19*$^{+/-}$ *Pim-1*$^{-/-}$) showed any detectable morphological or histopathological abnormalities in the BM or spleen. Next, we investigated peripheral blood from mice with the four different genotypes at 6-8 weeks of age for the standard parameters Hb, RBC, EVF, MCV, MCHC and WBC (table 1). The double mutant (*Rps19*$^{+/-}$ *Pim-1*$^{-/-}$) mice show increased RBC and WBC counts in peripheral blood when compared to the two single mutant (*Rps19*$^{+/-}$ *Pim-1*$^{+/+}$, *Rps19*$^{+/+}$ *Pim-1*$^{-/-}$) mice strains and wild type (*Rps19*$^{+/+}$ *Pim-1*$^{+/+}$). Microcytosis, which is associated with Pim-1 deficiency [18], was confirmed in the single *Pim-1*$^{-/-}$ mutant mice as well as the double mutant (*Rps19*$^{+/-}$ *Pim-1*$^{-/-}$) mice. Despite an increased RBC count, the double mutant mice display subnormal Hb and EVF which is less pronounced when compared to *Pim-1* deficient mice. These findings suggest that the interaction between RPS19 and PIM-1 [13] has an effect on proliferation and/or survival of RBC and WBC.

The increased myeloid cellularity in *Rps19*$^{+/-}$ *Pim-1*$^{-/-}$ mice is associated with an up-regulation of c-Myc. Neither Pim-1 deficiency nor Rps19 haploinsufficiency alone did result in

deregulation of c-Myc. It has been shown that c-Myc cooperates with Pim-1; Pim-1 phosphorylates histones required for c-Myc dependent transcription [20] and Pim-1 phosphorylates c-Myc itself [19]. In addition, c-Myc have been shown to directly promote ribosome biogenesis through the transcriptional regulation of ribosomal proteins, RNA polymerase I and III and factors involved in ribosome assembly [28,29]. On the other hand, c-Myc activity is suppressed by the ribosomal protein L11 [30] and by ribosomal protein L24 haploinsufficiency [31]. These results indicate a crosstalk between the c-Myc induced cell growth and the translational machinery. Thus, the increased levels of c-Myc observed in *Rps19*$^{+/-}$ *Pim-1*$^{-/-}$ mice may be related to a loss of a feedback mechanism involving both Rps19 and Pim-1.

c-Myc is essential for hematopoietic stem-cell renewal and cell progression [32]. In addition, c-Myc sensitizes cells to apoptosis through the mitochondrial apoptosis pathway. c-Myc primes a molecular switch of the Bcl-2 family of proteins resulting in a activation of the apoptotic factors Bak-Bax whereas the antagonistic factors Bcl_2, Bcl_{XL} and Mcl-1 are suppressed [33]. Over-expression of Bcl-2 has in early experiments shown to block c-Myc induced apoptosis without inhibiting cell cycle progression [34,35]. Unexpectedly, we observe an up-regulation of the anti-apoptotic factors Bcl_2, Bcl_{XL} and Mcl-1 in the double mutant (*Rps19*$^{+/-}$ *Pim-1*$^{-/-}$) mice. This was found associated with a down-regulation of the apoptotic protein Bak and the more downstream factor Caspase 3 consistent with the known inhibitory effects of Bcl_2, Bcl_{XL} and Mcl-1 on Bak-Bax. These findings indicate that the *Rps19*$^{+/-}$ *Pim-1*$^{-/-}$ mice has an altered balance between pro-apoptotic and anti-apoptotic Bcl family members resulting in reduced apoptosis.

c-Myc expression suppresses the cell cycle regulator p21 [36] and we confirmed a marked reduction of p21 levels in the *Rps19*$^{+/-}$ *Pim-1*$^{-/-}$ mice. The suppression of p21 in combination with the observed normal levels of p53 indicates that the BM cells are not under stress. The

promoting effect of c-Myc on cell cycle progression and cell growth together with the altered balance between Bcl-2 family of proteins may then result in the increased myeloid cellularity observed in *Rps19*$^{+/-}$ *Pim-1*$^{-/-}$ mice. From our results, we suggest an inter-dependent effect of *Rps19* and *Pim-1* as sensitizers in murine myeloid cell growth. We hypothesize that the combination of Rps19 insufficiency and Pim-1 deficiency result in the loss of a regulatory loop involving c-Myc. Simultaneously, *Rps19* insufficiency and *Pim-1* deficiency seems to suppress the c-Myc induced apoptotic switch. As a result, cell cycle progression and cell survival is promoted consistent with the increased peripheral cellularity observed in the *Rps19*$^{+/-}$*Pim-1*$^{-/-}$ mice.

In conclusion, our combined data show that allelic *Rps19* insufficiency and *Pim-1* deficiency have a co-operative effect on murine hematopoiesis resulting in an increased peripheral erythroid and myeloid cellularity. This is associated with deregulated c-Myc levels, expression of anti-apoptotic markers and suppression of p21. RPS19 insufficiency in DBA is associated with increased disposition for MDS and AML which presumably requires a combination of mutations. We suggest that candidate target genes in this progression encode cell cycle regulators or anti-apoptotic factors with functions analogous to those of PIM-1.

Acknowledgements

The authors wish to thank Prof. Helena Jernberg-Wiklund for valuable discussions and reagents. We also thank Prof. Fabrizio Loreni for the RPS19 antibody and Prof. Anton Berns for the *Pim-1*$^{-/-}$ mouse model.

Funding

This work was supported by grants from the Children's Cancer Foundation of Sweden, the DBA foundation, the Daniella and Maria Arturi foundation, the US National Institute of

Health (grant no. 5R01-HL079567-02), the Swedish Science Foundation, Uppsala University and Uppsala University Hospital.

Conflict-of-interest disclosure: The authors declare no competing financial interests.

References

1. Tamary H ,Alter BP. Current diagnosis of inherited bone marrow failure syndromes. *Pediatr Hematol Oncol* 2007 Mar; **24**(2)**:**87-99.
2. Alter B. Childhood red cell aplasia. *American Journal of Pediatric Hematology and Onccology* 1980**:**121-139.
3. Corey SJ, Minden MD, Barber DL, Kantarjian H, Wang JC ,Schimmer AD. Myelodysplastic syndromes: the complexity of stem-cell diseases. *Nat Rev Cancer* 2007 Feb; **7**(2)**:**118-129.
4. Ebert BL, Pretz J, Bosco J, Chang CY, Tamayo P, Galili N, *et al.* Identification of RPS14 as a 5q- syndrome gene by RNA interference screen. *Nature* 2008 Jan 17; **451**(7176)**:**335-339.
5. Draptchinskaia N, Gustavsson P, Andersson B, Pettersson M, Willig TN, Dianzani I, *et al.* The gene encoding ribosomal protein S19 is mutated in Diamond-Blackfan anaemia. *Nat Genet* 1999 Feb; **21**(2)**:**169-175.
6. Boria I, Quarello P, Avondo F, Garelli E, Aspesi A, Carando A, *et al.* A new database for ribosomal protein genes which are mutated in Diamond-Blackfan Anemia. *Hum Mutat* 2008 Sep 9; **29:** E263-E270.
7. Flygare J, Kiefer T, Miyake K, Utsugisawa T, Hamaguchi I, Da Costa L, *et al.* Deficiency of ribosomal protein S19 in CD34+ cells generated by siRNA blocks erythroid development and mimics defects seen in Diamond-Blackfan anemia. *Blood* 2005 Jun 15; **105**(12)**:**4627-4634.
8. Miyake K, Utsugisawa T, Flygare J, Kiefer T, Hamaguchi I, Richter J, *et al.* RPS19 Deficiency Leads to Reduced Proliferation and Increased Apoptosis but Does Not Affect Terminal Erythroid Differentiation in a Cell Line Model of Diamond-Blackfan Anemia. *Stem Cells* 2007 Oct 25; **26**(2)**:**323-329.
9. Ellis SR ,Lipton JM. Diamond Blackfan anemia: a disorder of red blood cell development. *Curr Top Dev Biol* 2008; **82:**217-241.
10. Flygare J, Aspesi A, Bailey JC, Miyake K, Caffrey JM, Karlsson S, *et al.* Human RPS19, the gene mutated in Diamond-Blackfan anemia, encodes a ribosomal protein required for the maturation of 40S ribosomal subunits. *Blood* 2007 Feb 1; **109**(3)**:**980-986.
11. Fodde R ,Smits R. Cancer biology. A matter of dosage. *Science* 2002 Oct 25; **298**(5594)**:**761-763.
12. Orru S, Aspesi A, Armiraglio M, Caterino M, Loreni F, Ruoppolo M, *et al.* Analysis of the ribosomal protein S19 interactome. *Mol Cell Proteomics* 2007 Mar; **6**(3)**:**382-393.
13. Chiocchetti A, Gibello L, Carando A, Aspesi A, Secco P, Garelli E, *et al.* Interactions between RPS19, mutated in Diamond-Blackfan anemia, and the PIM-1 oncoprotein. *Haematologica* 2005 Nov; **90**(11)**:**1453-1462.
14. Bachmann M ,Moroy T. The serine/threonine kinase Pim-1. *Int J Biochem Cell Biol* 2005 Apr; **37**(4)**:**726-730.
15. Amaravadi R ,Thompson CB. The survival kinases Akt and Pim as potential pharmacological targets. *J Clin Invest* 2005 Oct; **115**(10)**:**2618-2624.
16. Peltola KJ, Paukku K, Aho TL, Ruuska M, Silvennoinen O ,Koskinen PJ. Pim-1 kinase inhibits STAT5-dependent transcription via its interactions with SOCS1 and SOCS3. *Blood* 2004 May 15; **103**(10)**:**3744-3750.
17. Mikkers H, Nawijn M, Allen J, Brouwers C, Verhoeven E, Jonkers J, *et al.* Mice deficient for all PIM kinases display reduced body size and impaired responses to hematopoietic growth factors. *Mol Cell Biol* 2004 Jul; **24**(13)**:**6104-6115.

18. Laird PW, van der Lugt NM, Clarke A, Domen J, Linders K, McWhir J, *et al.* In vivo analysis of Pim-1 deficiency. *Nucleic Acids Res* 1993 Oct 11; **21**(20)**:**4750-4755.
19. Zhang Y, Wang Z, Li X ,Magnuson NS. Pim kinase-dependent inhibition of c-Myc degradation. *Oncogene* 2008 Aug 14; **27**(35)**:**4809-4819.
20. Zippo A, De Robertis A, Serafini R ,Oliviero S. PIM1-dependent phosphorylation of histone H3 at serine 10 is required for MYC-dependent transcriptional activation and oncogenic transformation. *Nat Cell Biol* 2007 Aug; **9**(8)**:**932-944.
21. Mochizuki T, Kitanaka C, Noguchi K, Muramatsu T, Asai A ,Kuchino Y. Physical and functional interactions between Pim-1 kinase and Cdc25A phosphatase. Implications for the Pim-1-mediated activation of the c-Myc signaling pathway. *J Biol Chem* 1999 Jun 25; **274**(26)**:**18659-18666.
22. Mochizuki T, Kitanaka C, Noguchi K, Sugiyama A, Kagaya S, Chi S, *et al.* Pim-1 kinase stimulates c-Myc-mediated death signaling upstream of caspase-3 (CPP32)-like protease activation. *Oncogene* 1997 Sep 18; **15**(12)**:**1471-1480.
23. Ruggero D ,Pandolfi PP. Does the ribosome translate cancer? *Nat Rev Cancer* 2003 Mar; **3**(3)**:**179-192.
24. Dai MS ,Lu H. Crosstalk between c-Myc and ribosome in ribosomal biogenesis and cancer. *J Cell Biochem* 2008 Oct 15; **105**(3)**:**670-677.
25. Matsson H, Davey EJ, Draptchinskaia N, Hamaguchi I, Ooka A, Leveen P, *et al.* Targeted disruption of the ribosomal protein S19 gene is lethal prior to implantation. *Mol Cell Biol* 2004 May; **24**(9)**:**4032-4037.
26. Matsson H, Davey EJ, Frojmark AS, Miyake K, Utsugisawa T, Flygare J, *et al.* Erythropoiesis in the Rps19 disrupted mouse: Analysis of erythropoietin response and biochemical markers for Diamond-Blackfan anemia. *Blood Cells Mol Dis* 2006 Mar-Apr; **36**(2)**:**259-264.
27. Nolan PM, Peters J, Strivens M, Rogers D, Hagan J, Spurr N, *et al.* A systematic, genome-wide, phenotype-driven mutagenesis programme for gene function studies in the mouse. *Nat Genet* 2000 Aug; **25**(4)**:**440-443.
28. Gomez-Roman N, Felton-Edkins ZA, Kenneth NS, Goodfellow SJ, Athineos D, Zhang J, *et al.* Activation by c-Myc of transcription by RNA polymerases I, II and III. *Biochem Soc Symp* 2006; (73)**:**141-154.
29. Boon K, Caron HN, van Asperen R, Valentijn L, Hermus MC, van Sluis P, *et al.* N-myc enhances the expression of a large set of genes functioning in ribosome biogenesis and protein synthesis. *EMBO J* 2001 Mar 15; **20**(6)**:**1383-1393.
30. Dai MS, Sears R ,Lu H. Feedback regulation of c-Myc by ribosomal protein L11. *Cell Cycle* 2007 Nov 15; **6**(22)**:**2735-2741.
31. Barna M, Pusic A, Zollo O, Costa M, Kondrashov N, Rego E, *et al.* Suppression of Myc oncogenic activity by ribosomal protein haploinsufficiency. *Nature* 2008 Dec 18; **456**(7224)**:**971-975.
32. Laurenti E, Varnum-Finney B, Wilson A, Ferrero I, Blanco-Bose WE, Ehninger A, *et al.* Hematopoietic stem cell function and survival depend on c-Myc and N-Myc activity. *Cell Stem Cell* 2008 Dec 4; **3**(6)**:**611-624.
33. Nieminen AI, Partanen JI ,Klefstrom J. c-Myc blazing a trail of death: coupling of the mitochondrial and death receptor apoptosis pathways by c-Myc. *Cell Cycle* 2007 Oct 15; **6**(20)**:**2464-2472.
34. Bissonnette RP, Echeverri F, Mahboubi A ,Green DR. Apoptotic cell death induced by c-myc is inhibited by bcl-2. *Nature* 1992 Oct 8; **359**(6395)**:**552-554.
35. Fanidi A, Harrington EA ,Evan GI. Cooperative interaction between c-myc and bcl-2 proto-oncogenes. *Nature* 1992 Oct 8; **359**(6395)**:**554-556.

36. Mukherjee S ,Conrad SE. c-Myc suppresses p21WAF1/CIP1 expression during estrogen signaling and antiestrogen resistance in human breast cancer cells. *J Biol Chem* 2005 May 6; **280**(18)**:**17617-17625.

Table 1. Peripheral blood parameters from adult mice with the genotypes *Rps19*$^{+/+}$ *Pim-1*$^{+/+}$ (w.t.), *Rps19*$^{+/-}$ *Pim-1*$^{+/+}$, *Rps19*$^{+/+}$*Pim-1*$^{-/-}$, *Rps19*$^{+/-}$ *Pim-1*$^{-/-}$.

	Mean value ± SD in mice (n)[a]			
	Rps19$^{+/+}$*Pim-1*$^{+/+}$	*Rps19*$^{+/-}$*Pim-1*$^{+/+}$	*Rps19*$^{+/+}$*Pim-1*$^{-/-}$	*Rps19*$^{+/-}$*Pim-1*$^{-/-}$
RBC[c] (10^{12}cells/L)	9,55±0,56 (22)	9,87±0,53 (13)	9,70±0,53 (25)	10,02±0,39 (23)[b]
WBC[c] (10^{9}cells/L)	4,75±1,33 (22)	5,92±2,63 (13)	5,20±1,45 (25)	6,06±1,88 (23)[b]
Hb[c] (g/L)	154,50±9,38 (22)	154,75±8,04 (13)	142,35±6,36 (25)[b]	146,90±5,18 (23)[b]
EVF[c]	0,51±0,03 (22)	0,52±0,02 (13)	0,48±0,03 (25)[b]	0,49±0,03 (23)[b]
MCV[c] (fL)	53,24±2,30 (22)	52,50±2,07 (13)	48,96±2,85 (25)[b]	49,13±3,00 (23)[b]
MCHC[c] (g/L)	304,15±9,83 (22)	300,54±9,24 (13)	301,44±13,34 (25)	299,00±11,48 (23)

[a] SD, standard deviation; n, number of mice analyzed.
[b] $P < 0.05$ (two-tailed unpaired student *t*-test compared to wild type).
[c] Abbreviations: RBC, red blood cell count; WBC, white blood cell count; Hb, hemoglobin; EVF, hematocrit; MCV, mean corpuscular volume; MCHC, mean corpuscular hemoglobin concentration.

Figure 1. Analysis of cell cycle regulators in mice BM cells. Western blot analysis of total BM proteins. Each protein measurement was normalized to beta-actin. Blots with mean values ±std from at least two independent measurements are shown. (A) c-Myc levels is significantly up-regulated (** $p<0.01$) in the double mutant (*Rps19*$^{+/-}$ *Pim-1*$^{-/-}$) mice when compared to the other three groups. (B) p21 levels is significantly down-regulated (* $p<0.05$) in the double mutant (*Rps19*$^{+/-}$ *Pim-1*$^{-/-}$) mice when compared to w.t. mice. (C) No altered p53 levels are found.

Figure 2. Analysis of apoptotic markers in mice BM cells. Western blot analysis of total BM proteins. Each protein measurement was normalized to beta-actin. Blots with mean values ±std from at least two independent measurements are shown. (A) The anti-apoptotic marker, Bcl_2, was found significantly up-regulated (* $p<0.05$) in the double mutant (*Rps19*$^{+/-}$ *Pim-1*$^{-/-}$) mice when compared to w.t. and *Rps19*$^{+/-}$ *Pim-1*$^{+/+}$ mice. (B) The anti-apoptotic marker, Mcl-1, was found significantly up-regulated (* $p<0.05$) in the double mutant (*Rps19*$^{+/-}$ *Pim-1*$^{-/-}$) mice when compared to w.t. and *Rps19*$^{+/-}$ *Pim-1*$^{+/+}$ mice. (C) The anti-apoptotic marker, Bcl_{XL}, was found significantly up-regulated (* $p<0.05$) in the double mutant (*Rps19*$^{+/-}$ *Pim-1*$^{-/-}$) mice when compared to w.t. mice. (D) The pro-apoptotic marker, Bak, was found significantly down-regulated (*** $p<0.001$) in the double mutant (*Rps19*$^{+/-}$ *Pim-1*$^{-/-}$) mice when compared to the other three groups. (E) The pro-apoptotic marker, cleaved Caspase 3, was found significantly down-regulated (* $p<0.05$) in the double mutant (*Rps19*$^{+/-}$ *Pim-1*$^{-/-}$) mice when compared to w.t. and *Rps19*$^{+/+}$ *Pim-1*$^{-/-}$ mice.

A

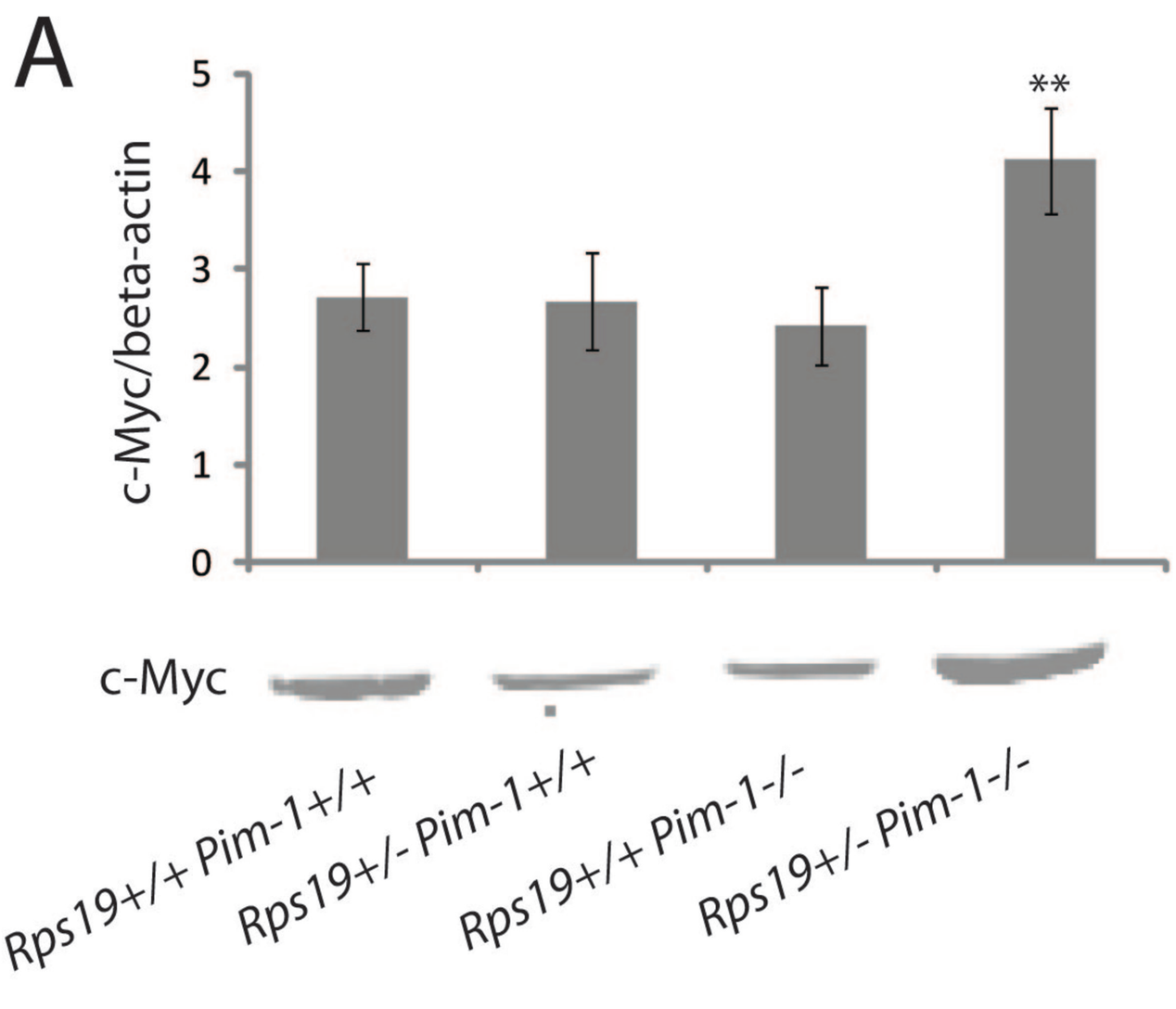
c-Myc/beta-actin
5
4
3
2
1
0
**
c-Myc
Rps19+/+ Pim-1+/+
Rps19+/- Pim-1+/+
Rps19+/+ Pim-1-/-
Rps19+/- Pim-1-/-

B

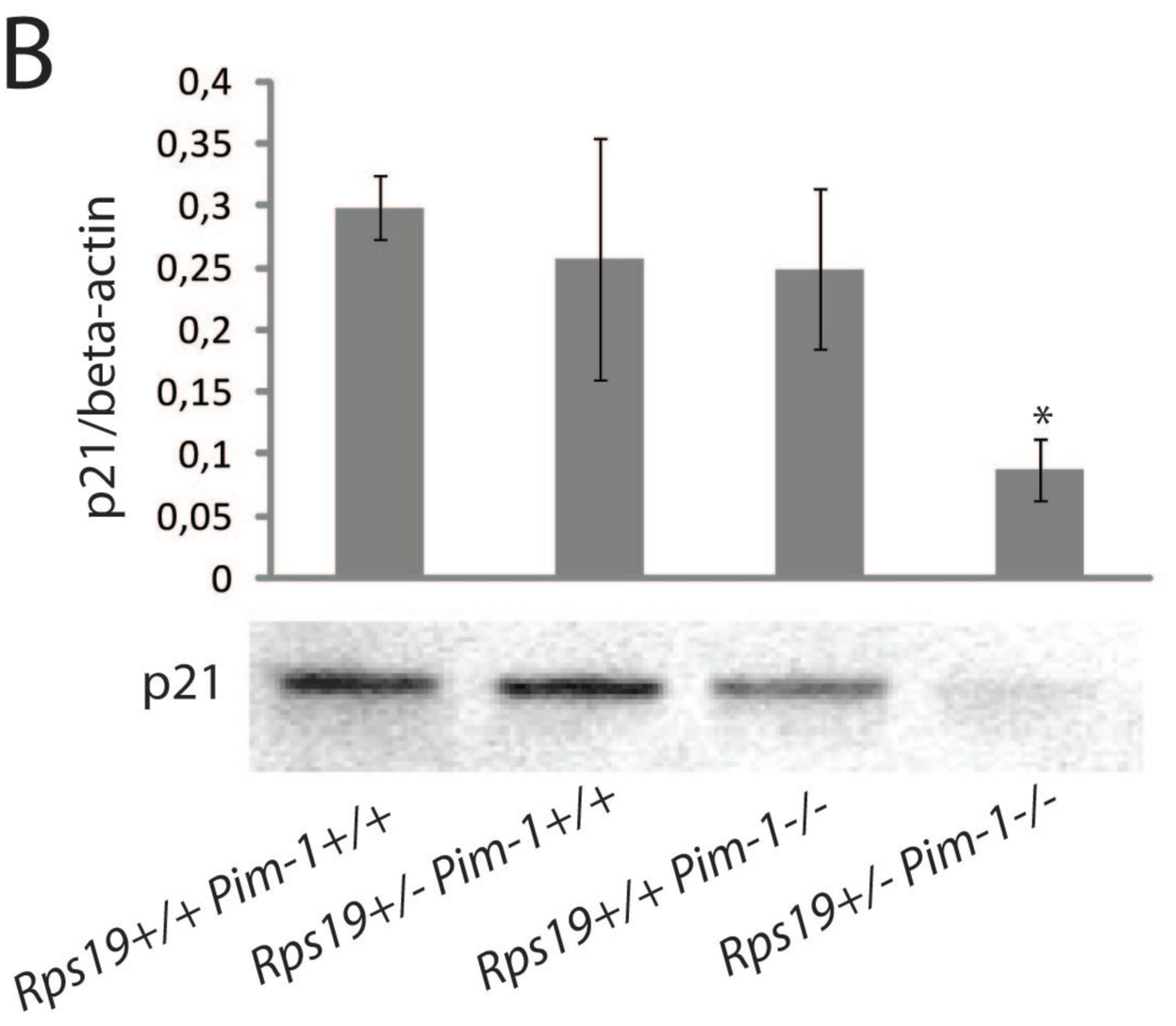
p21/beta-actin
0,4
0,35
0,3
0,25
0,2
0,15
0,1
0,05
0
*
p21
Rps19+/+ Pim-1+/+
Rps19+/- Pim-1+/+
Rps19+/+ Pim-1-/-
Rps19+/- Pim-1-/-

C

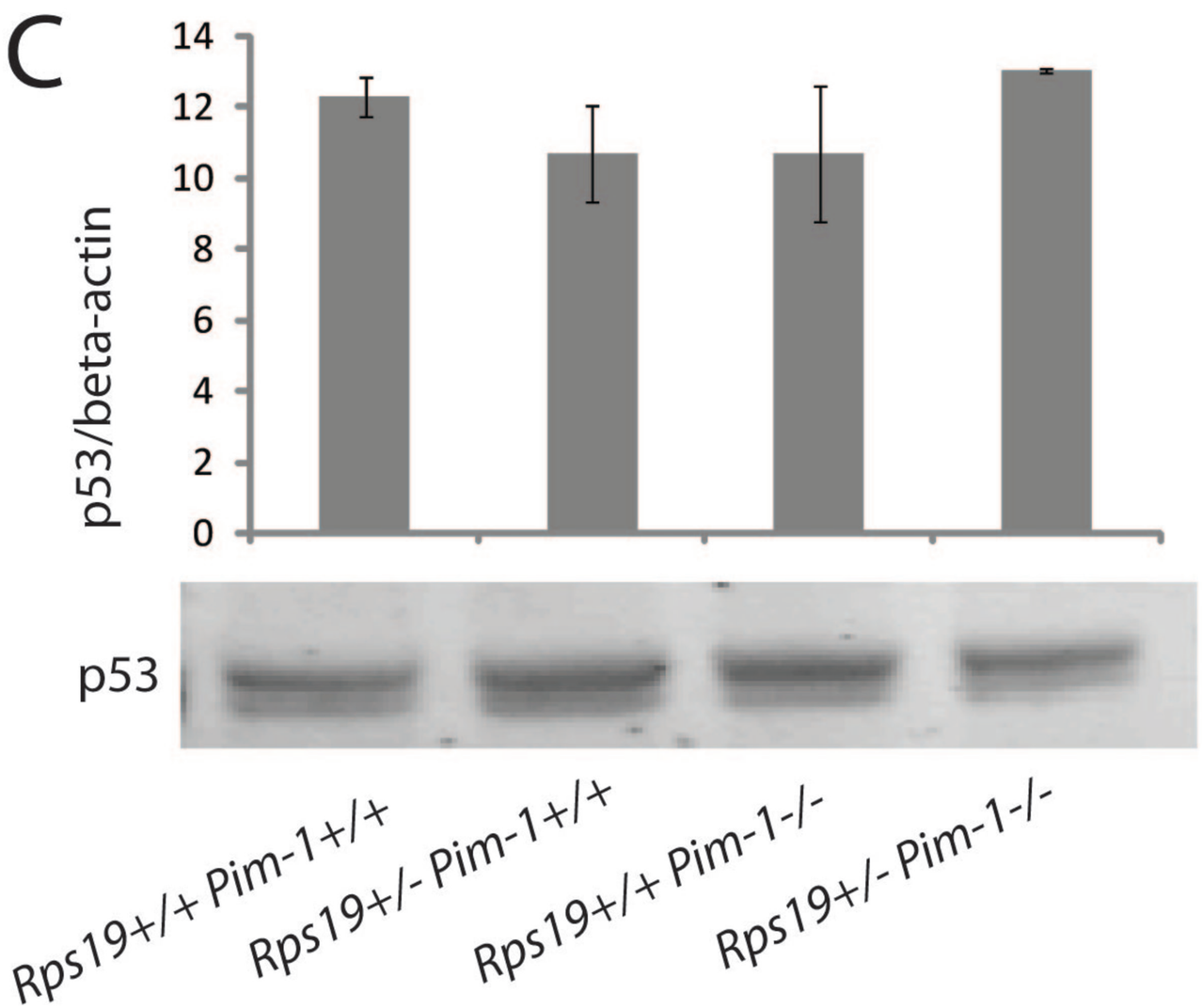
p53/beta-actin
14
12
10
8
6
4
2
0
p53
Rps19+/+ Pim-1+/+
Rps19+/- Pim-1+/+
Rps19+/+ Pim-1-/-
Rps19+/- Pim-1-/-

A

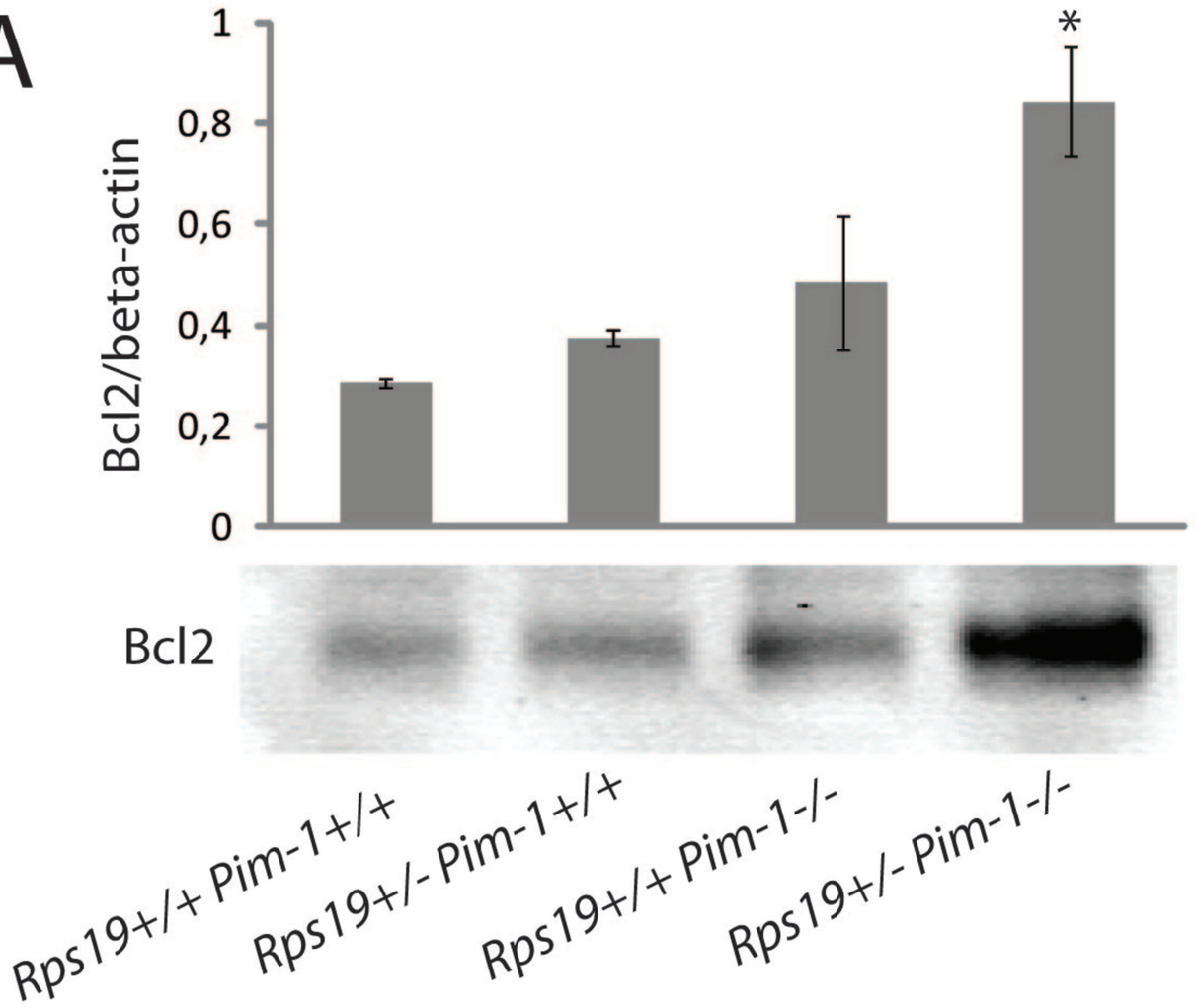
Bcl2/beta-actin
1
0,8
0,6
0,4
0,2
0
*
Bcl2
Rps19+/+ Pim-1+/+
Rps19+/- Pim-1+/+
Rps19+/+ Pim-1-/-
Rps19+/- Pim-1-/-

B

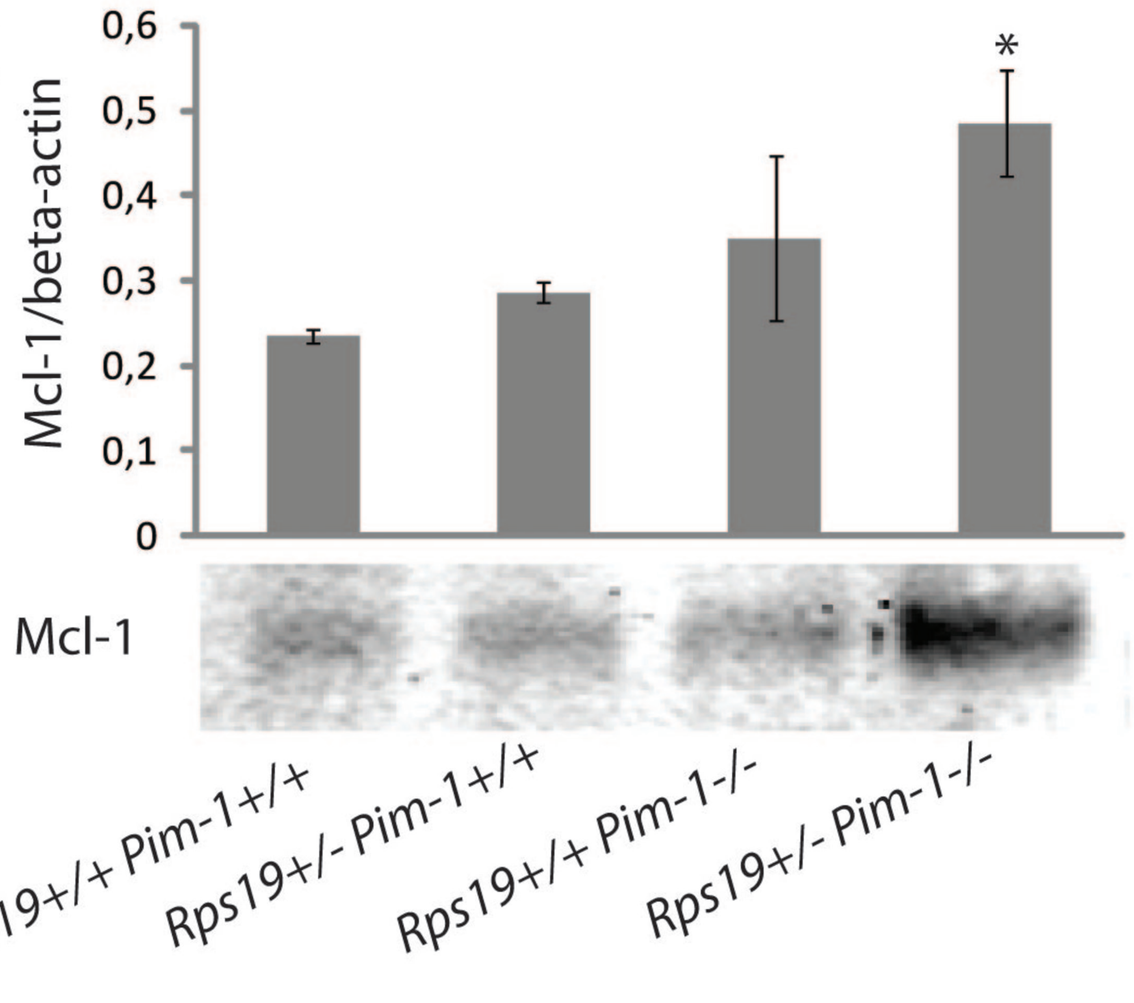
Mcl-1/beta-actin
0,6
0,5
0,4
0,3
0,2
0,1
0
*
Mcl-1
Rps19+/+ Pim-1+/+
Rps19+/- Pim-1+/+
Rps19+/+ Pim-1-/-
Rps19+/- Pim-1-/-

C

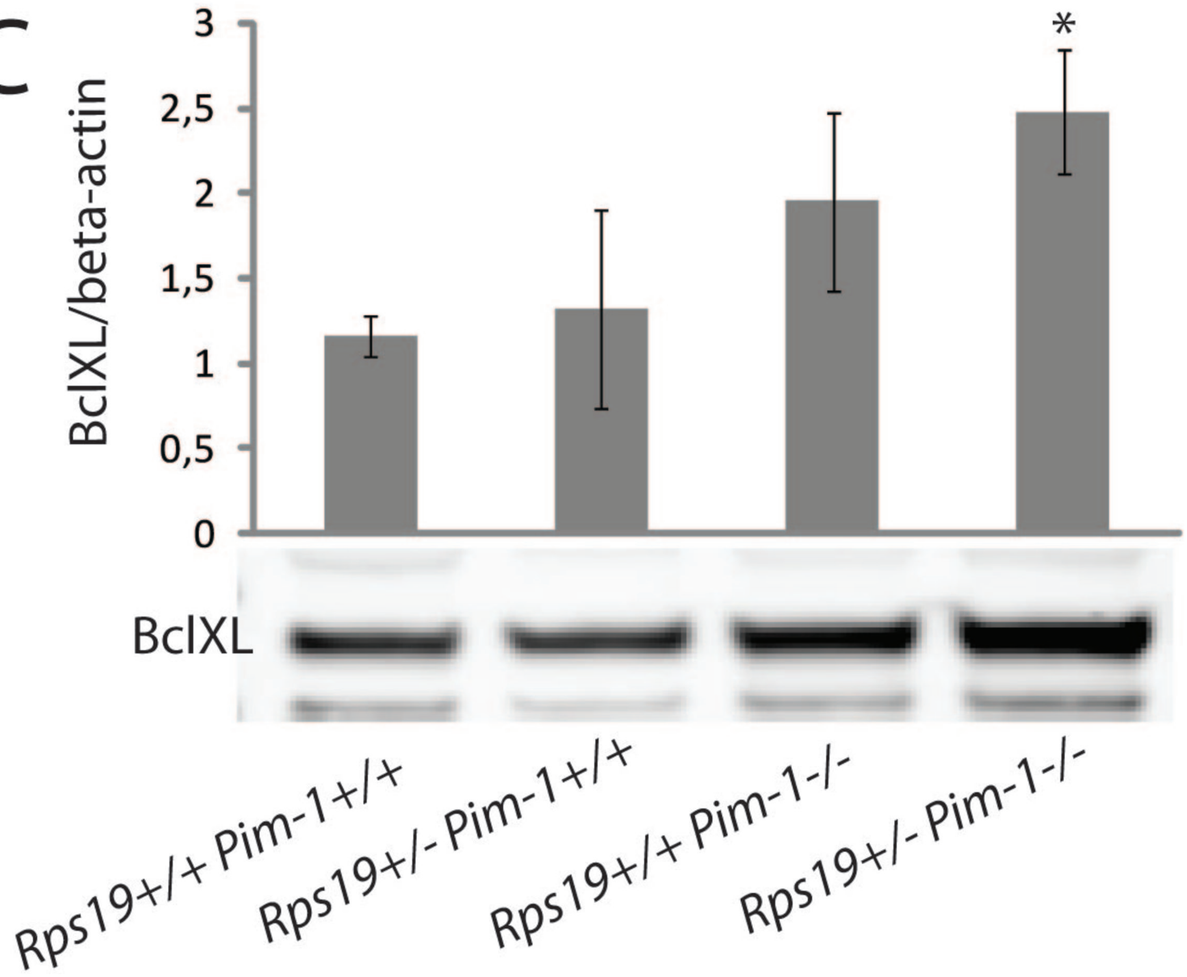
BclXL/beta-actin
3
2,5
2
1,5
1
0,5
0
*
BclXL
Rps19+/+ Pim-1+/+
Rps19+/- Pim-1+/+
Rps19+/+ Pim-1-/-
Rps19+/- Pim-1-/-

D

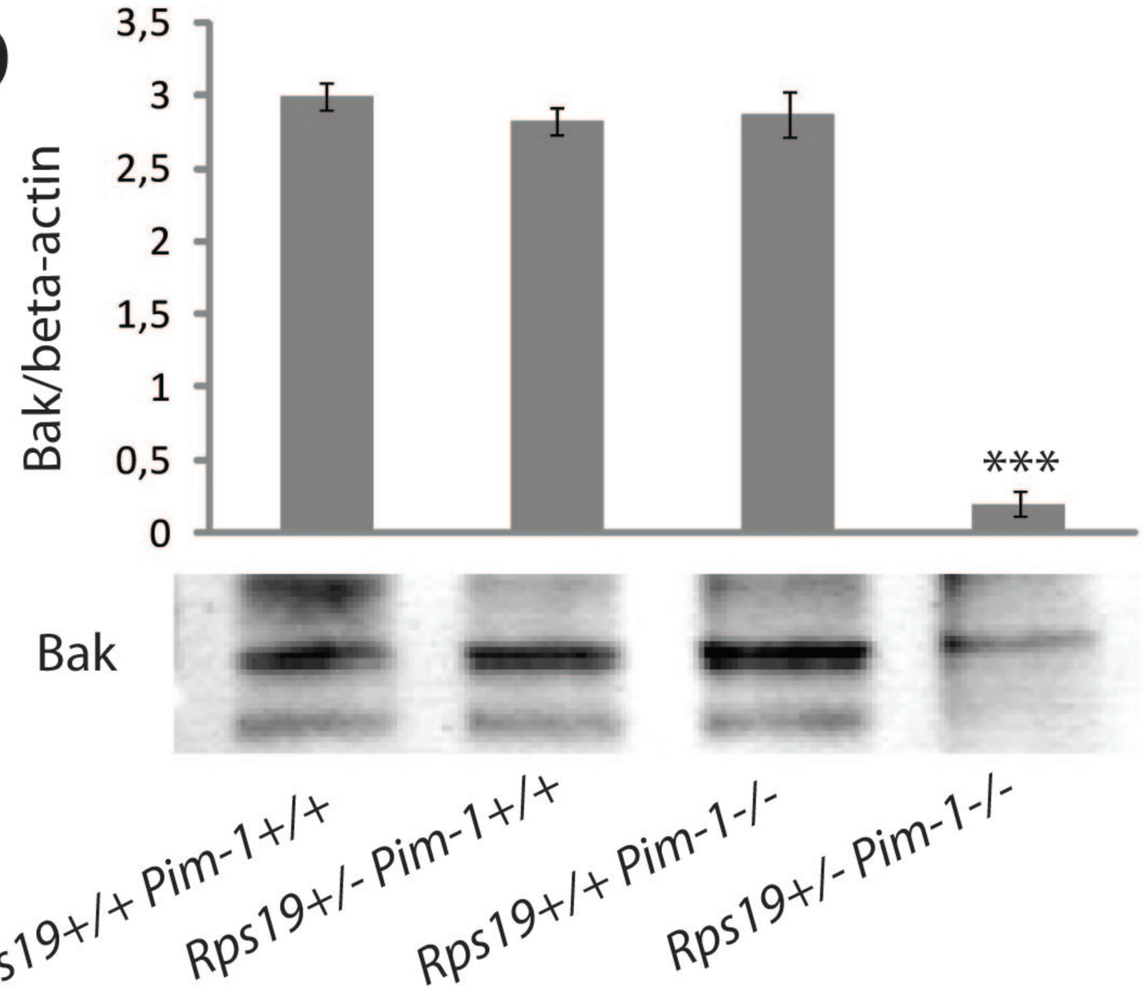
Bak/beta-actin
3,5
3
2,5
2
1,5
1
0,5
0
***
Bak
Rps19+/+ Pim-1+/+
Rps19+/- Pim-1+/+
Rps19+/+ Pim-1-/-
Rps19+/- Pim-1-/-

E

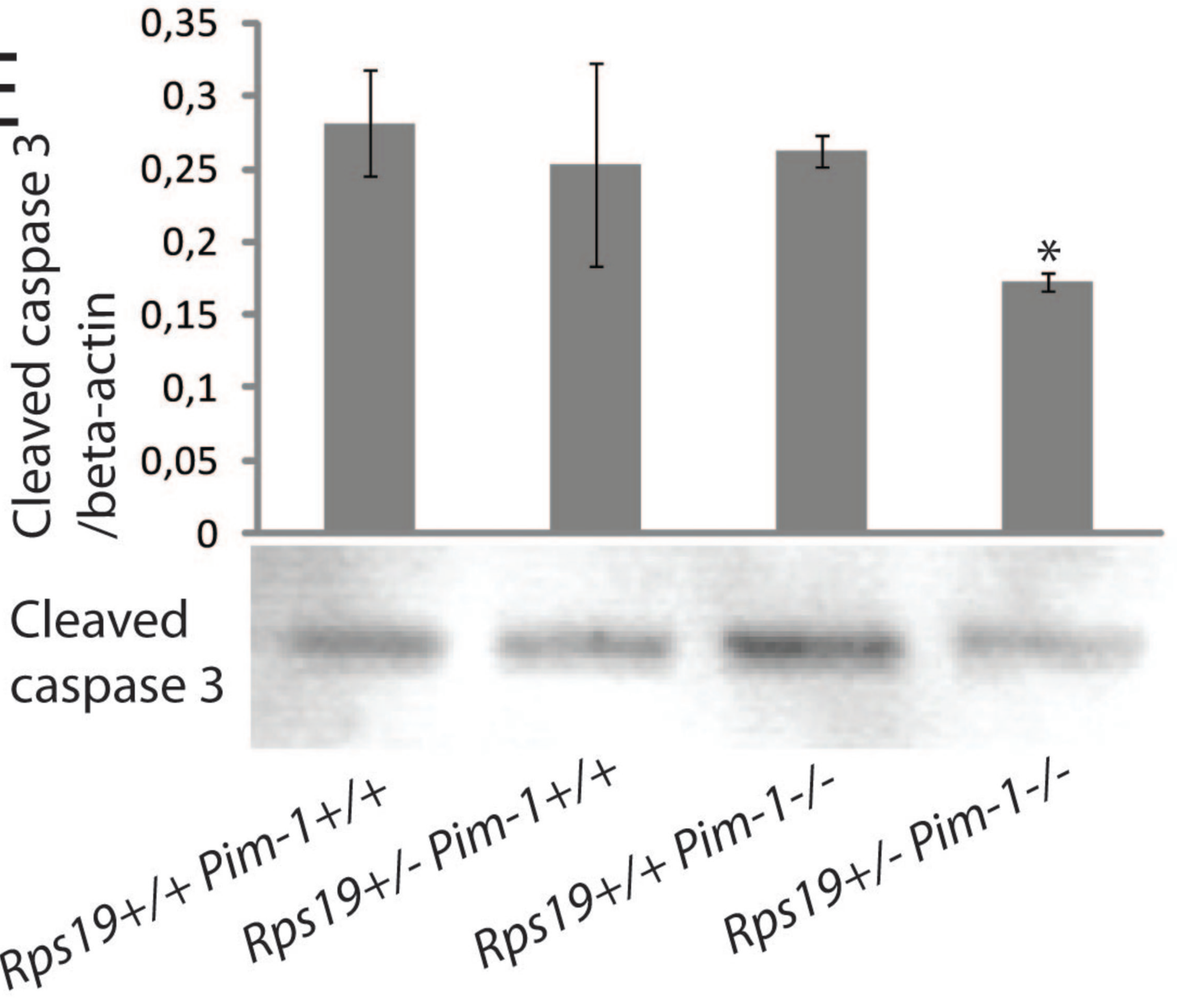
Cleaved caspase 3
/beta-actin
0,35
0,3
0,25
0,2
0,15
0,1
0,05
0
*
Cleaved
caspase 3
Rps19+/+ Pim-1+/+
Rps19+/- Pim-1+/+
Rps19+/+ Pim-1-/-
Rps19+/- Pim-1-/-